

Assessment of Pile Vibrations in Various Soil Layers

Dilshod Kholikov^{1, a)}, Dilfuza Ismatova^{2, b)} Elbek Ismoilov^{3, c)},
Kamola Khaydarova^{3, d)}

¹Zarmed University Samarkand compus, Samarkand, Uzbekistan

²Samarkand State University of Architecture and Construction, Samarkand, Uzbekistan

³Samarkand State University, 140104, University blv. 15, Samarkand city, Uzbekistan

^{a)} dilshodxoliqov2587@gmail.com

^{b)} ismatovadilfuza12@gmail.com

^{c)} eismoilov.samsu@gmail.com

^{d)} Corresponding author: xaydarovakamolaxakimovna@gmail.com

Abstract. The calculation of pile foundations should be carried out using mathematical models that describe their mechanical behavior. The design scheme can be represented both in analytical and numerical forms. When determining the bearing capacity and settlement of single piles, preference should be given to tabulated or analytical solutions provided in construction standards and regulations. All calculations of piles, pile foundations, and their bases should be performed using the design values of material and soil properties. This paper presents the results of an assessment of the influence of the excitation frequency of the pile foundation base on the amplitudes of transverse vibrations of a pile interacting with a two-layer soil according to the Winkler model.

INTRODUCTION

According to the provisions of SNIP II-7-81 “*Construction in Seismic Regions*”, the design model of the “pile–soil medium” system [1] must be selected taking into account the most significant factors that determine the stress state and deformations of the foundation and structural elements of the building (the structural scheme of the building, construction features, the nature of soil layers, the properties of foundation soils, and the possibility of their changes during construction and operation, etc.).

When designing pile foundations, the following factors should be taken into account: soil conditions of the construction site, hydrogeological regime, features of pile installation, and the presence of slurry beneath the pile tips. The design values of soil properties should be determined in accordance with **GOST 20522**, and the design values of the subgrade reaction coefficients of the soil surrounding the pile - in accordance with **Appendix [1]**.

Studies [2-5] present analyses and results of investigations on pile foundations interacting with various types of collapsible soils. The main requirements for pile foundation structures are outlined in manuals [6-8]. The methodology for calculating pile foundations under the influence of seismic waves and kinematic excitations is described in works [9].

In this paper, the vibration process of a pile foundation interacting with the base according to the **Winkler model**, where the base undergoes kinematic excitation, is considered.

PROBLEM STATEMENT

Let us set the origin of coordinates at the lower cross-section of the beam and direct the *OX* axis vertically upward. Let $W_1(x, t)$ and $W_2(x, t)$ denote the deflections of the beam in each zone (Figure 1), which satisfy the following equations

$$EJ \frac{\partial^4 W_1}{\partial x^4} + m \frac{\partial^2 W_1}{\partial t^2} + k_1 W_1 = 0 \text{ for } 0 < x < l \quad (1)$$

$$EJ \frac{\partial^4 W_2}{\partial x^4} + m \frac{\partial^2 W_2}{\partial t^2} + k_2 W_2 = 0 \text{ for } l < x < L \quad (2)$$

The functions $W_1(x, t)$ and $W_2(x, t)$ satisfy the following boundary conditions

$$\frac{\partial W_1}{\partial x} = 0, \quad EJ \frac{\partial^3 W_1}{\partial x^3} = k_0(W_1 - W_0) \text{ at } x = 0 \quad (3)$$

$$\frac{\partial^2 W_1}{\partial x^2} = 0, \quad EJ \frac{\partial^3 W_1}{\partial x^3} = M \frac{\partial^2 W_1}{\partial t^2} \text{ at } x = L \quad (4)$$

under compatibility conditions

$$\begin{cases} W_1 = W_2, \quad \frac{\partial W_1}{\partial x} = \frac{\partial W_2}{\partial x}, \\ \frac{\partial^2 W_1}{\partial x^2} = \frac{\partial^2 W_2}{\partial x^2}, \quad \frac{\partial^3 W_1}{\partial x^3} = \frac{\partial^3 W_2}{\partial x^3} \end{cases} \text{ at } x = l \quad (5)$$

where k_0 is the stiffness coefficient of the contact during shear at the lower cross-section of the beam with the base, which moves according to the law $W_0 = W_0(t)$, M is the mass of the attached body (pile cap) at the upper cross-section of the beam.

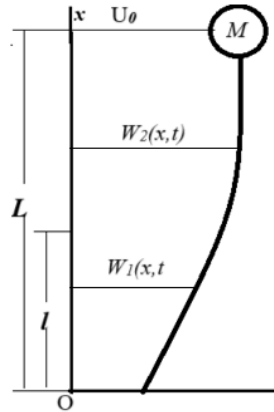


FIGURE 1. Scheme of the transverse bending of a beam carrying a concentrated mass M . Here, EJ is the flexural rigidity of the beam, m is the mass per unit length, k_1 and k_2 are the subgrade reaction coefficients for each zone of beam-soil contact, with corresponding lengths l and $L-l$, and L is the total length of the beam.

We assume $W_0(t) = U_0 \sin \omega t$ (U_0 - amplitude, ω - frequency) and represent the solutions of equations (1) and (2) in the form of

$$W_1 = U_1(x) \sin \omega t, \quad W_2 = U_2(x) \sin \omega t$$

where the functions $U_1(x)$ and $U_2(x)$ satisfy the equations

$$EJ U_1'''' + (k_1 - m\omega^2) U_1 = 0 \quad 0 < x < l \quad (6)$$

$$EJ U_2'''' + (k_2 - m\omega^2) U_2 = 0 \quad l < x < L \quad (7)$$

boundary

$$U_1'(0) = 0, \quad EJ U_1'''(0) = k_0[U_1(0) - U_0] \quad (8)$$

$$U_2''(L) = 0, \quad EJ U_2'''(L) = -M\omega^2 U_2(L) \quad (9)$$

matching conditions

$$U_1(l) = U_2(l), \quad U_1'(l) = U_2'(l), \quad U_1''(l) = U_2''(l), \quad U_1'''(l) = U_2'''(l) \quad (10)$$

METHOD OF SOLUTION

When performing the calculations, we assume that $k_1 \geq 4k_2$

1. We consider the case $\omega < \sqrt{k_2/m}$ (Case 1).

The general solution of equations (6) and (7) can be written as:

$$U_1 = C_1 Y_1(\beta_1 * (\xi - l1)) + C_2 Y_2(\beta_1 * (\xi - l1)) + C_3 Y_3(\beta_1 * (\xi - l1)) + C_4 Y_4(\beta_1 * (\xi - l1))$$

$$U_2 = C_1 S_1[\beta_2(\xi - l1)] + C_2 \frac{\beta_1}{\beta_2} S_2[\beta_2(\xi - l1)] + B_3 \frac{\beta_1^2}{\beta_2^2} S_3[\beta_2(\xi - l1)] + B_4 \frac{\beta_1^3}{\beta_2^3} S_4[\beta_2(\xi - l1)]$$

$$\text{where } w = \sqrt{\frac{m\omega^2 L^4}{EJ}}, \quad \beta_1 = \sqrt[4]{w_1^2 - w^2}, \quad \beta_2 = \sqrt[4]{w_2^2 - w^2}, \quad w_1 = \sqrt{\frac{k_1 L^4}{4EJ}}, \quad w_2 = \sqrt{\frac{k_2 L^4}{EJ}}, \quad l_1 = l/L.$$

$Y_1(\beta z), S_1(\beta z)$ are Krylov functions [5], defined by the formulas:

$$\begin{aligned} Y_1 &= \cos \beta_1 z \operatorname{ch} \beta_1 z, & Y_2 &= (\sin \beta_1 z \operatorname{ch} \beta_1 z + \cos \beta_1 z \operatorname{sh} \beta_1 z), \\ Y_3 &= \sin \beta_1 z \operatorname{sh} \beta_1 z, & Y_4 &= (\sin \beta_1 z \operatorname{ch} \beta_1 z - \cos \beta_1 z \operatorname{sh} \beta_1 z), \\ S_1 &= \cos \beta_2 z \operatorname{ch} \beta_2 z, & S_2 &= (\sin \beta_2 z \operatorname{ch} \beta_2 z + \cos \beta_2 z \operatorname{sh} \beta_2 z), \\ S_3 &= \sin \beta_2 z \operatorname{sh} \beta_2 z, & S_4 &= (\sin \beta_2 z \operatorname{ch} \beta_2 z - \cos \beta_2 z \operatorname{sh} \beta_2 z). \end{aligned}$$

The constants C_1, C_2, C_3 and C_4 are determined from conditions (8)-(10), which yield:

$$\begin{aligned} C_1 &= \frac{-\beta_0^2 S_{12}}{d_0}, & C_2 &= \frac{\beta_0^2 S_{11}}{d_0}, \\ C_3 &= C_1 r_{11} + C_2 r_{12}, & C_4 &= C_1 r_{21} + C_2 r_{22}, \\ s_{21} &= a_{21} + r_{11} a_{23} + r_{21} a_{24}, & s_{22} &= a_{22} + r_{12} a_{23} + r_{22} a_{24}, \\ d_0 &= s_{11} s_{22} - s_{12} s_{21}, & s_{11} &= a_{11} + r_{11} a_{13} + r_{21} a_{14}, & s_{12} &= a_{12} + r_{12} a_{13} + r_{22} a_{14}, \\ r_{11} &= \frac{b_{21} b_{14} - b_{11} b_{24}}{d}, & r_{12} &= \frac{b_{22} b_{14} - b_{12} b_{24}}{d}, & d_0 &= b_{13} b_{24} - b_{23} b_{14} \\ r_{21} &= \frac{b_{11} b_{23} - b_{21} b_{13}}{d}, & r_{22} &= \frac{b_{12} b_{23} - b_{22} b_{13}}{d}, \\ b_{21} &= \alpha w^2 S_1(1, w) + b_{01} S_3(1, w), & b_{22} &= \alpha w^2 S_2(1, w) \frac{\beta_1}{\beta_2} + b_{02} S_4(1, w), \\ b_{23} &= \alpha w^2 S_3(1, w) \frac{\beta_1^2}{\beta_2^2} + b_{03} S_2(1, w), & b_{22} &= \alpha w^2 S_4(1, w) \frac{\beta_1^3}{\beta_2^3} + b_{04} S_1(1, w), \\ b_{01} &= -2\beta_2^3, & b_{02} &= -4\beta_2^2 \beta_1, & b_{03} &= -2\beta_2^2 \beta_2, & b_{04} &= 4\beta_1^3, \\ b_{11} &= -\beta_2^3 S_3(1, w), & b_{12} &= -\beta_2^2 \beta_1 S_4(1, w), & b_{13} &= \beta_1^2 \beta_2 S_1(1, w), & b_{14} &= \beta_1^3 S_2(1, w), \\ a_{21} &= -2\beta_1^3 Y_2(0, w) + \beta_0^2 Y_1(0, w), & a_{22} &= -4\beta_1^3 Y_3(0, w) + \beta_0^2 Y_2(0, w), \\ a_{23} &= -2\beta_1^3 Y_4(0, w) + \beta_0^2 Y_3(0, w), & a_{24} &= 4\beta_1^3 Y_1(0, w) + \beta_0^2 Y_4(0, w) \\ a_{11} &= -\beta_1 Y_4(0, w), & a_{12} &= 2\beta_1 Y_1(0, w), & a_{13} &= \beta_1 Y_2(0, w), & a_{14} &= 2\beta_1 Y_3(0, w). \end{aligned}$$

RESULTS

The calculations were carried out for the following parameter values:

$$\begin{aligned} E &= 2 \cdot 10^{11} \text{Pa}, & a &= 0.3 \text{m}, & h &= 0.3 \text{m}, & L &= 5 \text{m}, & \rho_0 &= 45 \frac{\text{kg}}{\text{m}}, & M &= 3000 \text{kg}, \\ k_1 &= 5 \cdot 10^6 \frac{\text{N}}{\text{m}^2}, & k_2 &= 10^6 \frac{\text{N}}{\text{m}^2}, & k_0 &= 5 \cdot 10^5 \frac{\text{N}}{\text{m}^2}. \end{aligned}$$

Figure 2 shows the curves of deflection and axial stress $\sigma = Eh \frac{d^2 U}{dx^2}$ distributions along the beam length $\xi = x/L$ for various values of the frequency ω .

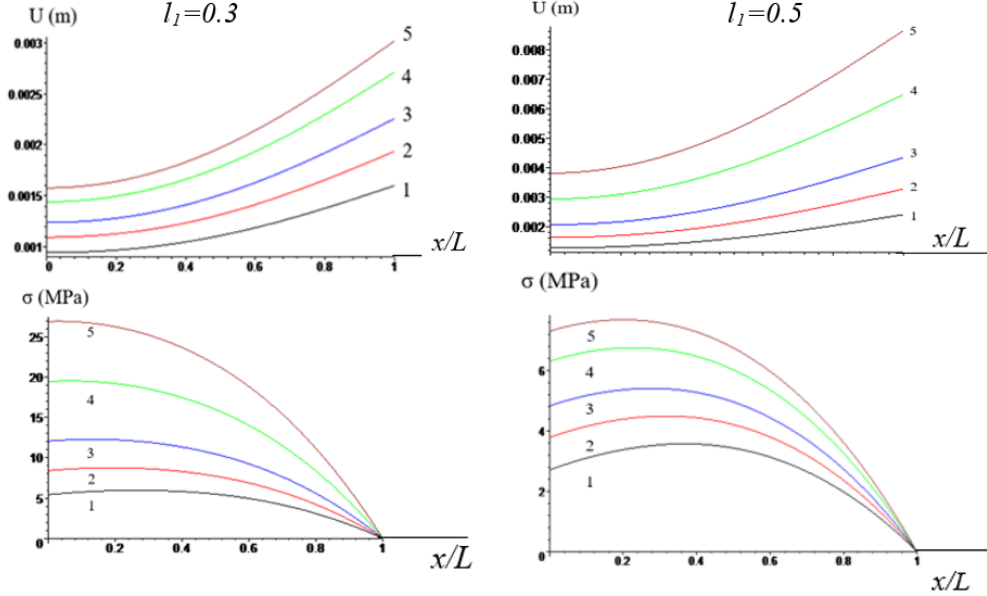


FIGURE 2. Curves of the distribution of the deflection amplitude $U(\text{m})$ and axial stress σ (MPa) along the beam length $\xi = x/L$ for two values of the ratio $l_1 = \frac{l}{L}$, at different values of the base vibration frequency $\omega(\text{sek}^{-1})$: 1- $\omega = 1.75$, 2- $\omega = 1.78$, 3- $\omega = 1.8$; 4- $\omega = 1.82$; 5- $\omega = 1.83$

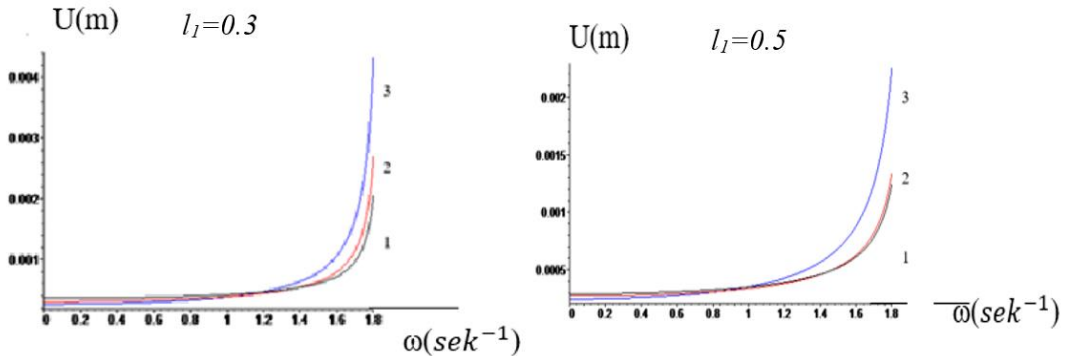


FIGURE 3. Dependence of the deflection amplitude $U(\text{m})$ on the frequency $\omega(\text{sek}^{-1})$ at sections $x = 0$ (curve 1), $x = l$ (curve 2), and $x = L$ (curve 3) for two values of the ratio $l_1 = \frac{l}{L}$

2. Let $\sqrt{\frac{k_2}{m}} < \omega < \sqrt{\frac{k_1}{4m}}$ (Case 2).

In this case, the general solution of equations (6) and (7) can be written as:

$$U_1 = C_1 Y_1(\beta_1 \cdot (\xi - l_1)) + C_2 Y_2(\beta_1 \cdot (\xi - l_1)) + C_3 Y_3(\beta_1 \cdot (\xi - l_1)) + C_4 Y_4(\beta_1 \cdot (x - l_1))$$

$$U_2 = C_1 S_1[\beta_2(\xi - l_1)] + C_2 \frac{\beta_1}{\beta_2} S_2[\beta_2(\xi - l_1)] + C_3 \frac{\beta_1^2}{\beta_2^2} S_3[\beta_2(\xi - l_1)] + C_4 \frac{\beta_1^3}{\beta_2^3} S_4[\beta_2(\xi - l_1)]$$

where, $\beta_1 = \sqrt[4]{w_1^2 - w^2}$, $\beta_2 = \sqrt[4]{w^2 - w_2^2}$. $Y_i(\beta z)$, $S_i(\beta z)$ are Krylov functions [5], defined by the following formulas:

$$\begin{aligned} Y_1 &= \cos \beta_1 z \operatorname{ch} \beta_1 z, & Y_2 &= (\sin \beta_1 z \operatorname{ch} \beta_1 z + \cos \beta_1 z \operatorname{sh} \beta_1 z), \\ Y_3 &= \sin \beta_1 z \operatorname{sh} \beta_1 z, & Y_4 &= (\sin \beta_1 z \operatorname{ch} \beta_1 z - \cos \beta_1 z \operatorname{sh} \beta_1 z), \\ S_1 &= 0.5(\operatorname{ch} \beta_2 z + \cos \beta_2 z), & S_2 &= 0.5(\operatorname{sh} \beta_2 z + \sin \beta_2 z), \\ S_3 &= 0.5(\operatorname{ch} \beta_2 z - \cos \beta_2 z), & S_4 &= 0.5(\operatorname{sh} \beta_2 z - \sin \beta_2 z). \end{aligned}$$

The constants C_1, C_2, C_3 and C_4 are determined from conditions (8)-(10).

Figure 4 shows the curves of deflection distribution along the beam length $\xi = x/L$ for various values of the frequency ω .

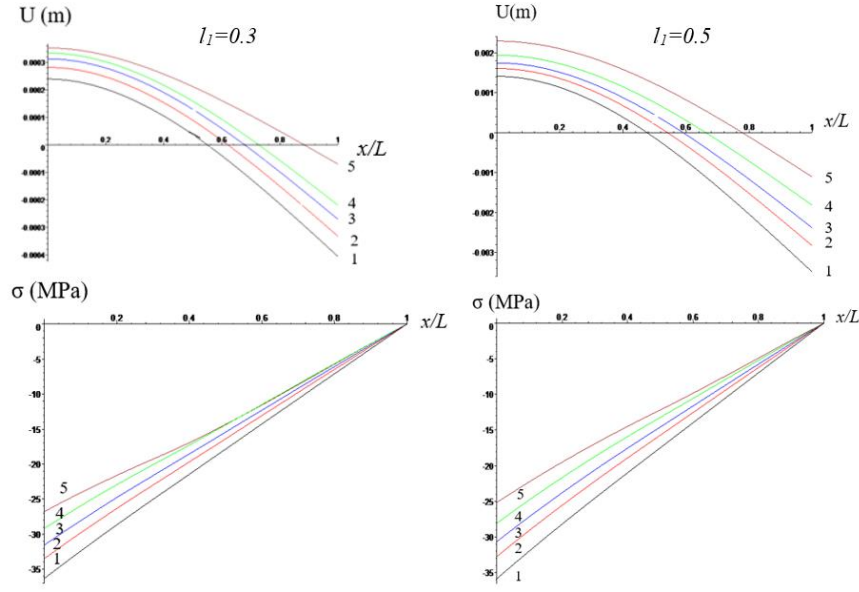


FIGURE 4. Curves of the deflection $U(m)$ and axial stress σ (MPa) distribution along the beam length $\xi = x / L$ for two values of the ratio $l_1 = \frac{l}{L}$ at different values of the base vibration frequency $\omega \left(\frac{1}{\text{sek}} \right)$: $1-\omega = 2.2, 2-\omega = 2.3, 3-\omega = 2.4, 4-\omega = 2.6, 5-\omega = 3.2$

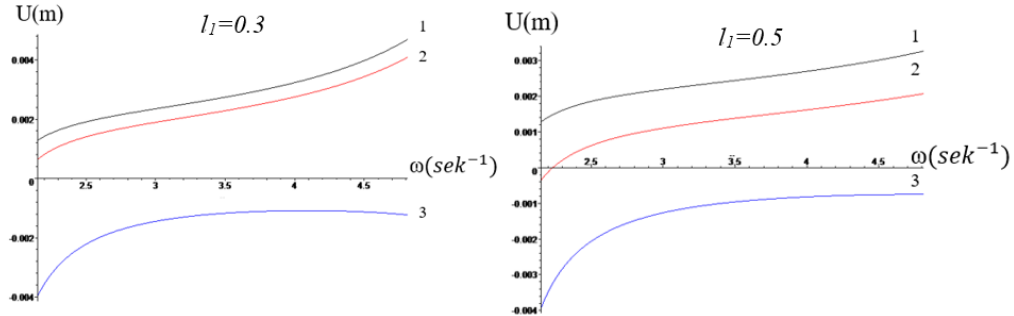


FIGURE 5. Dependence of the deflection amplitude on the frequency $\omega \left(\frac{1}{\text{sek}} \right)$ at sections $x = 0$ (curve 1), $x = l$ (curve 2), and $x = L$ (curve 3) for two values of the ratio $l_1 = \frac{l}{L}$

3. Now consider the case where the external excitation frequency satisfies the inequality $\omega > \sqrt{\frac{k_1}{4m}}$ (Case 3).

In this case, the general solution of equations (6) and (7) can be written as:

$$U_1 = C_1 Y_1(\beta_1 * (\xi - l1)) + C_2 Y_2(\beta_1 * (\xi - l1)) + C_3 Y_3(\beta_1 * (\xi - l1)) + C_4 Y_4(\beta_1 * (\xi - l1))$$

$$U_2 = C_1 S_1[\beta_2(\xi - l1)] + C_2 \frac{\beta_1}{\beta_2} S_2[\beta_2(\xi - l1)] + C_3 \frac{\beta_1^2}{\beta_2^2} S_3[\beta_2(\xi - l1)] + C_4 \frac{\beta_1^3}{\beta_2^3} S_4[\beta_2(\xi - l1)]$$

where, $\beta_1 = \sqrt[4]{w^2 - w_1^2}$, $\beta_2 = \sqrt[4]{w^2 - w_2^2}$,

$Y_i(\beta z)$, $S_i(\beta z)$ are Krylov functions [5], defined by the formulas:

$$Y_1 = 0.5 * (ch\beta_1 z + \cos \beta_1 z), \quad Y_2 = 0.5 * (sh\beta_1 z + \sin \beta_1 z),$$

$$Y_3 = 0.5 * (ch\beta_1 z - \cos \beta_1 z), \quad Y_4 = 0.5 * (sh\beta_1 z - \sin \beta_1 z),$$

$$S_1 = 0.5 * (ch\beta_2 z + \cos \beta_2 z), \quad S_2 = 0.5 * (sh\beta_2 z + \sin \beta_2 z),$$

$$S_3 = 0.5 * (ch\beta_2 z - \cos \beta_2 z), \quad S_4 = 0.5 * (sh\beta_2 z - \sin \beta_2 z).$$

The constants C_1, C_2, C_3 and C_4 are determined from conditions (8)-(10).

Figure 6 shows the curves of deflection distribution along the beam length for various values of the frequency ω .

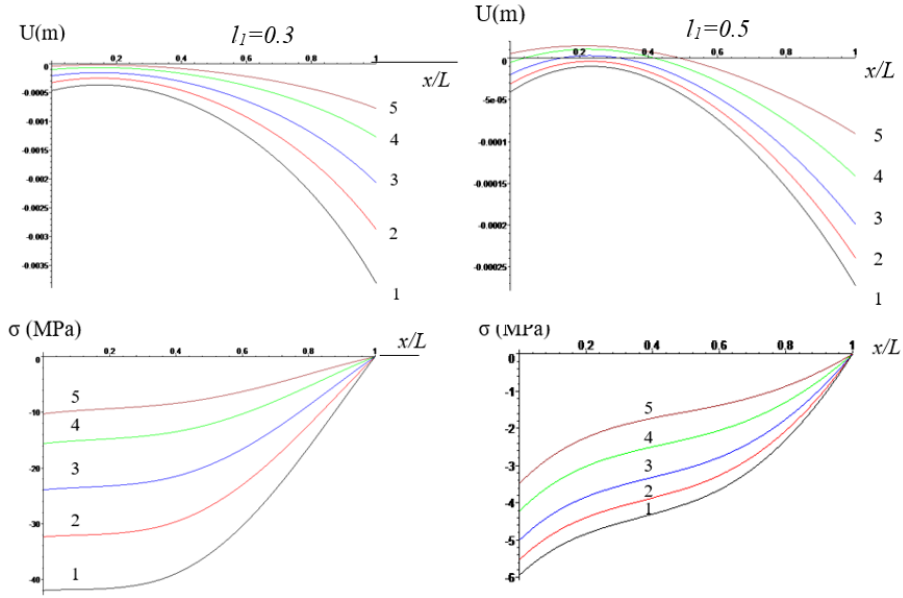


FIGURE 6. Curves of the deflection amplitude $U(m)$ and axial stress σ (MPa) along the beam length $\xi = x/L$ for two values of the ratio $l_1 = \frac{l}{L}$ at different base vibration frequencies ω ($\frac{1}{\text{sek}}$): 1- $\omega = 4$, 2- $\omega = 4.2$, 3- $\omega = 4.5$; 4- $\omega = 4.6$; 5- $\omega = 5$

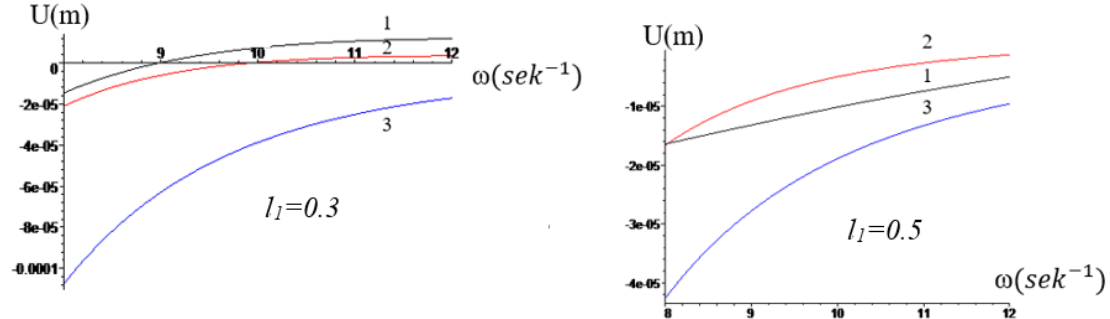


FIGURE 7. Dependence of the deflection amplitude on the frequency $\omega(\text{sek}^{-1})$ at sections $x=0$ (curve 1), $x=L$ (curve 2), and $x=L$ (curve 3) for two values of the ratio $l_1 = \frac{l}{L}$.

CONCLUSION

Analysis of the results shows a significant influence of external excitation frequencies close to resonance on the magnitudes of beam deflections and axial stresses. At low frequencies (Figure 2), near the resonance frequency ($1.72 < \omega < 2$), the beam deflections along its length increase monotonically and reach high values as the frequency approaches resonance. In this case, the tensile stresses attain their maximum values at the lower section of the beam.

For frequencies in the range $\sqrt{\frac{k_2}{m}} < \omega < \sqrt{\frac{k_1}{4m}}$ (Case 2), the pattern of deflections and stresses changes: the deflections of the upper section can become negative, and the entire length of the beam is under compression.

Finally, at high values of the external excitation frequency (Figure 6, Case 3), the beam also remains in compression, with deflections along the entire length being practically negative, and the largest deflections occurring at the section where the mass is attached. Increasing the length of the contact zone l between the two soil conditions leads to a reduction in both deflections and stress values along the beam.

REFERENCES

1. Pile Foundations. Updated Edition of SNiP 2.02.03-85. Official Edition. Moscow, (2011).
2. A.A. Grigoryan, Pile Foundations of Buildings and Structures on Collapsible Soils, Moscow, Stroyizdat, (1984).

3. V.A. Ilyichev, Geotechnical Handbook: Foundations, Substructures, and Underground Structures. Moscow, ASV Publishing, (2014).
4. A.T. Iovchuk, On the Use of Piles in Soils with Weak Layers, Foundations and Mechanics of Soils, **2**, 32–36 (1967).
5. R.A. Mangushev, Modern Pile Technologies: Textbook, 2nd edition, 2010.
6. Guidelines for Designing Pile Foundations of Buildings and Structures on Collapsible Soils. Moscow, Stroyizdat, (1969).
7. R.A. Mangushev, Piles and Pile Foundations: Structures, Design, and Technologies, Moscow, ASV, (2015).
8. Guidelines for Designing Pile Foundations. Moscow, NIIOSP named after N.M. Gersevanov, (1980).
9. A.G. Bulgakov, Formulation and Solution of the Problem of Interaction of Building Structures on Pile Foundations with Seismic Waves, Theory of Engineering Structures, Building Constructions, **2**, 3–13 (2014).